Proceedings of the 2nd International Symposium
on Adaptive Motion of Animals and Machines,
Kyoto, March.4-8, 2003

Measurement and Numerical Simulation of a Flapping Butterfly

Kei SENDA[1], **Tsuyoshi TANAKA**[2], **and Masakazu SAWAMOTO**[3]

[1]Kanazawa Univ., 2-40-20 Kodatsuno, Kanazawa, Ishikawa 920-8667, Japan, senda.k@t.kanazawa-u.ac.jp

[2]Formor Graduate Student, Osaka Prefecture Univ.

[3]Undergraduate Student, Kanazawa Univ.

Abstract

This paper is concerned with the flapping of wings of a butterfly, which is rhythmic and cyclic motion. The objective is to clarify the principle of a stable flapping-of-wings flight. First, a dynamics model of a butterfly is derived for analyses by Lagrange's method, where the butterfly is considered as a rigid body system. Second, a simple method and a vortex method are applied to make a simulator where the methods calculates the aerodynamic force. Next, a experimental system with a low-speed wind tunnel is constructed for fundamental data of flapping-of-wings motion, where the system measures the aerodynamic force and the motion simultaneously by a balance and a optical measurement system. Validity of the mathematical model is examined by comparing the measured data with the numerical results. A periodic orbit of a flapping-of-wings flight is searched so as to fly the butterfly model. Furthermore, numerical computation examines the stability of a flapping-of-wings motion generated by a neural network oscillator.

1. Introduction

Rhythmic and cyclic motions are observed in locomotion, flapping, and swimming of animals and insects. Although living things cannot repeat the same movement with sufficient accuracy unlike robots, they can maintain desired movement stably against environmental uncertainty and variations because of their adaptation-capability. The objective of this study is to clarify the principle of stabilization of motion in living animals. A prospective target may be applications of the principle to intelligent motion control of robots. Concretely, this study considers a flapping-of-wings flight of a butterfly, which is a rhythmical periodic motion, and tries to clarify the principle that enables the flight.

The flapping-of-wings flight of a butterfly might be realized by intricately-intertwining with many factors, i.e., movement of the mass center of the butterfly, air flow over wings, leading edge vortexes, and so on. There are many unknown points for the stable flight, e.g., "how the butterfly moves," "whether feedback control is used," etc. These unknowns must be clarified.

For the purpose, research is advanced in the following plan:

1. deriving of dynamics model and simulator construction,
2. the experimental measurement of the motions of butterflies and aerodynamic forces,
3. discussions for the stable flapping-of-wings flight through the simulator.

The rest of this paper is organized as follows. A butterfly is considered as a rigid multi-body system, and a dynamics model is developed by Lagrange's method in section 2. For aerodynamic forces, a simple method and a vortex method are introduced to build a simulator. In section 3, an experimental system with a low-speed wind tunnel is constructed for fundamental data acquisition of flapping-of-wings motion, where the system measures aerodynamic force and motion simultaneously by a balance and a optical measurement system. Validity of the mathematical model is examined by comparing the measured data with the numerical results. According to the comparison, the computation methods are reviewed in section 4. A periodic orbit of a flapping-of-wings flight is described by using a neural network, and the periodic target orbit of the flapping is searched in section 5 so as to fly the butterfly model. Furthermore, numerical simulations examines that the butterfly model can fly by flapping-of-wings motion generated by the neural network oscillator. Finally, concluding remarks are given by section 6.

2. Mathematical Model of Butterfly

2.1. Rigid multibody system

A butterfly is modeled by a multi-body system with 4 links as shown in Fig. 1 (a), which is composed of

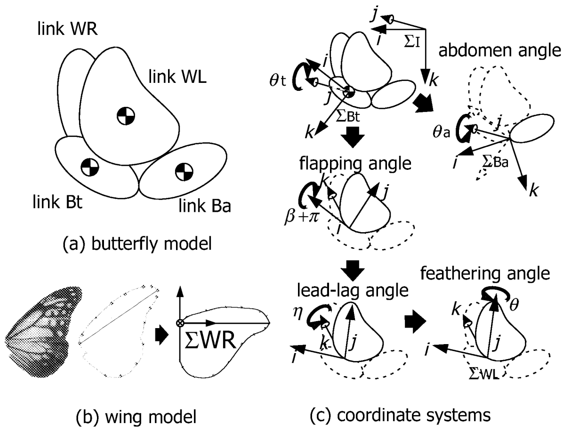

Figure 1: Modeling of a butterfly

Table 1: Characteristics of a butterfly

Parameters		Values	
Total mass	M	0.238×10^{-3}	kg
Aspect ratio	AR	4.0676	
Wing loading	Mg/S_W	0.987846	Nm^{-2}
Thorax mass	m_{Bt}	0.095×10^{-3}	kg
Thorax length	$2l_{Bt}$	15×10^{-3}	m
Thorax width	$2w_{Bt}$	8×10^{-3}	m
Abdomen mass	m_{Ba}	0.105×10^{-3}	kg
Abdomen length	$2l_{Ba}$	20×10^{-3}	m
Abdomen width	w_{Ba}	5×10^{-3}	m
Wing mass	m_W	0.019×10^{-3}	kg
Wing length	y_{tip}	0.049	m
Wing area	S_W	0.118×10^{-2}	m^2

the thorax Bt considered as a main body, the abdomen Ba, the left wings WL, and right wings WR. Both the model and its motions are supposed to be symmetrical. A pair of fore and hind wings of each side is modeled by a panel as shown in Fig. 1 (b). The following equations of motion are obtained by using Lagrange's method:

$$(\boldsymbol{M} - \boldsymbol{F}_s)\ddot{\boldsymbol{\theta}} + \dot{\boldsymbol{M}}\dot{\boldsymbol{\theta}} - \frac{1}{2}\frac{\partial}{\partial \boldsymbol{\theta}}\left(\dot{\boldsymbol{\theta}}^T \boldsymbol{M}\dot{\boldsymbol{\theta}}\right) + \frac{\partial V}{\partial \boldsymbol{\theta}} - \boldsymbol{\tau}_{sv} - \boldsymbol{\tau}_d = \boldsymbol{\tau}_{control} \quad (1)$$

where the generalized coordinates are $\boldsymbol{\theta} = [x\ z\ \theta_t\ \theta_a\ \beta\ \eta\ \theta]^T$. As illustrated in Fig. 1 (c), x, z, and θ_t are x, y-positions and attitude angle of the thorax, β flapping angle in up-down direction, η lead-lag angle, θ feathering angle representing torsion angle. The $\boldsymbol{M}$ and V are the inertia matrix and a potential energy, respectively. The terms $\boldsymbol{F}_s\ddot{\boldsymbol{\theta}} + \boldsymbol{\tau}_{sv}$ and $\boldsymbol{\tau}_d$ of the aerodynamic force will be developed in the following section.

An actual butterfly, Parantica sita niphonica, will be used for experiments in a later section. Specifications of the butterfly are listed in Table 1.

2.2. Fundamental computation methods for aerodynamics

2.2.1. Simple method

In this study, we use two computation methods for fundamental aerodynamic forces applied to wings, e.g., a simple method and a vortex method. Here, at first, the simple method is introduced. Though the simple method is literally simple, it is expected to be comparatively well in agreement with complicated 3-dimensional calculation methods[1].

This method considers that the aerodynamic force to a wing is given by the sum of $\boldsymbol{F}_s\ddot{\boldsymbol{\theta}}+\boldsymbol{\tau}_{sv}$ and $\boldsymbol{\tau}_d$, where the former is aerodynamic force of the additional mass, which is a mass of fluid moving with the wing and the latter is a function of the flow velocity.

The simple method regards that $\boldsymbol{\tau}_d$ is proportional to dynamic pressure. This method divides a wing into thin strip elements along the wingspan. A strip element is applied by an aerodynamic force

$$df_z = \frac{1}{2}\rho v_z^2 C_n dS \quad (2)$$

where dS is the area of the strip element, ρ mass density of fluid, v_z flow velocity perpendicular to the strip element, and C_n a coefficient of lift. The aerodynamic force perpendicular to the wing is given by

$$f_z = \int df_z \quad (3)$$

In the meantime, the aerodynamic force parallel to the wing is

$$f_x = k f_z \quad (4)$$

where k gives a rate of f_x to f_z. The parameters C_n and k are determined by experimental results.

2.2.2. Vortex method

As the second method for the aerodynamic forces, a vortex method is introduced, which is referred as a lumped vortex method in [2]. This method also considers an aerodynamic force as the sum of $\boldsymbol{F}_s\ddot{\boldsymbol{\theta}} + \boldsymbol{\tau}_{sv}$ and $\boldsymbol{\tau}_d$. The former is computed as same as the simple method, whereas $\boldsymbol{\tau}_d$ is computed by the following method.

This method also divides a wing into thin strip elements along the wingspan. Then $\boldsymbol{\tau}_d$ is computed by the

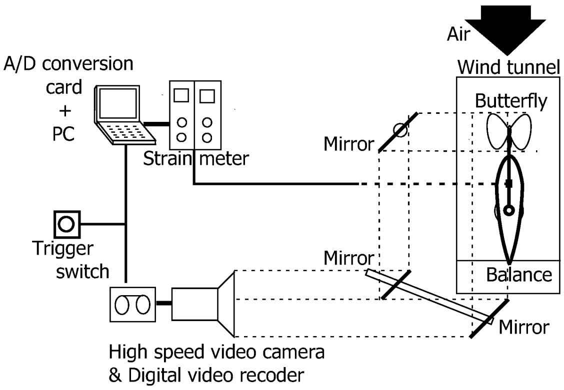

Figure 2: Experimental setup

sum of the aerodynamic forces applied to all the thin strip elements. The vortex method allocates a bound vortex to the each strip element, decides its strength so as to satisfy the Kutta condition at trailing edge, and obtains aerodynamic forces using the two-dimensional potential flow theorem.

Viscosity effect should be contained in the model because of the low Reynolds number $Re \simeq 10^3$ for the butterfly. However, the computed viscous drag is approximately 0.5% of the maximum drag. As a result, the potential flow theorem may result in good agreement with the real flow since the viscous effect is negligible.

3. Experiments of Flapping-of-Wings

3.1. Outline of experimental system

Verification of the models and parameter setting require fundamental data of flapping-of-wings motions and aerodynamic forces. For the purpose, an experimental system with a low-speed wind tunnel is constructed and a wind tunnel experiment is conducted using an actual butterfly, Parantica sita niphonica.

The simultaneous measurement system is constructed as illustrated in Fig. 2, which measures the motion and the forces applied to the butterfly using an optical measurement system and a force measurement system with a balance. The butterfly is gummed up on the back of the thorax to the tip of the balance. The balance with the butterfly is put into the wind tunnel, the flapping-of-wings motion in the flow is captured on videotape, and the state vector $\boldsymbol{\theta}$ is measured using the video images. Simultaneously, the forces applied to the butterfly are measured by the balance.

3.2. Optical motion measurement

Fig. 2 shows that the side and the back views of the flapping-of-wings motion are captured on videotape simultaneously by using three mirrors and a video camera. Frame rate is 125 frames par second for about 6 Hz of flapping-of-wings frequency of the butterfly. For the motion measurement, a frozen image is made for each frame. Cartesian coordinates of four marked points are calculated from the image. The points are the fixed point on the back of the thorax to the tip of the balance, the back end of the abdomen, the tip of the fore wing, and a point on the hind wing. Because the thorax is fixed, its position and orientation are constant.

3.3. Force measurement

A balance is hand-made to measure small dynamic forces below 10^{-1} N. Three components of the applied force at the fixed point to the tip of the balance are measured, i.e., the lift L in $\boldsymbol{i}_I$ direction, the drag D in $\boldsymbol{k}_I$ direction, and the force moment M in $\boldsymbol{j}_I$ direction about the fixed point.

The butterfly and balance can be regarded as a vibration system with a mass, i.e., the butterfly, at the tip of a cantilever beam. Its measured eigen frequency is 52.3 Hz, and the small oscillation is mixed in the measured signals. The oscillation is cleaned-up from the measurements by using a low-pass filter whose cut-off frequency is 30 Hz for about 6 Hz of flapping-of-wings frequency. Consequently, the force measurement system has guaranteed the flat gain characteristic and no phase shifting up to 30 Hz.

In addition, the video camera and the PC for force measurement start at the same instant by a trigger signal.

3.4. Experiments

3.4.1. Measured results

An experiment is conducted under a condition that the main flow is 1 m/s, the thoracic positions $x = z = 0$ m, and its angle $\theta_t = 31°$. Figs. 3 and 4 are the experimental results measured by the above optical and force measurement system.

Fig. 3 illustrates the $\boldsymbol{\theta}$ measured by the optical system. The butterfly repeats this periodic motion for about 0.16 seconds when it continues the steady flapping-of-wings motion. If the rigid multibody model of the butterfly runs with the trajectory of Fig. 3, the right-and-left wings collide with each other after

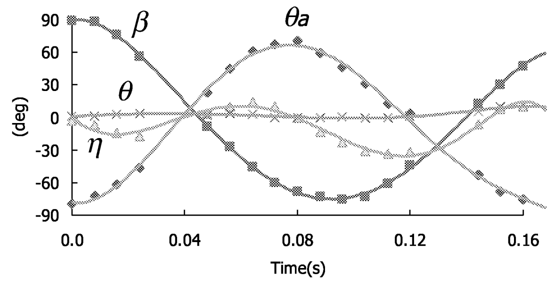

Figure 3: Experimental measurements of generalized coordinates

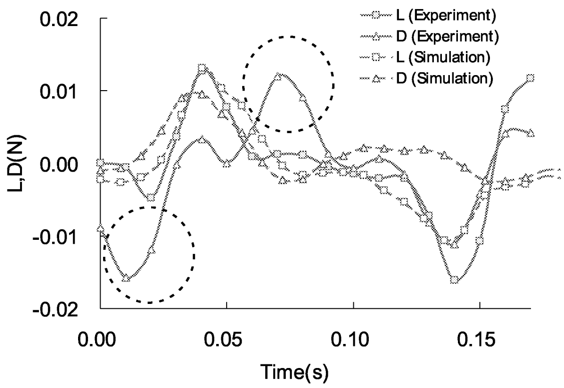

Figure 4: Lift and drag of actual butterfly and model

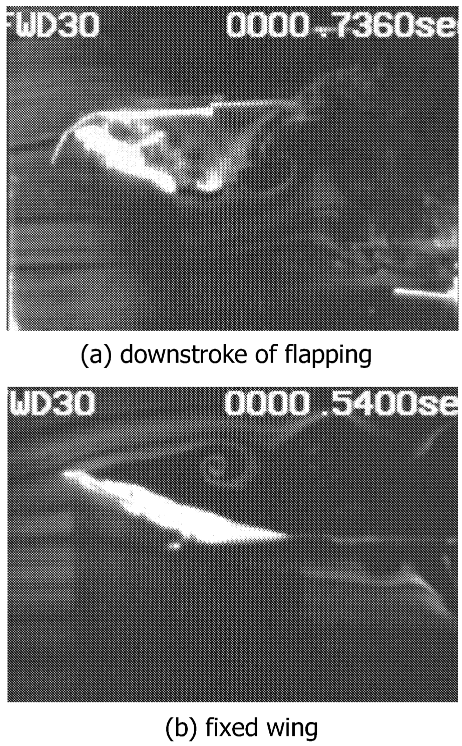

Figure 5: Visualized flow around flapping and fixed wings

the downstroke about $t = 0.08$ s. The actual butterfly adjusts the overlapping of the fore and the hind wings, and controls wing chord length. A hard collision is avoided by together with the elastic deformation of wings, even though the real right-and-left wings almost contact with each other.

Fig. 4 shows the measured forces at the tip of the balance, i.e., the lift L, the drag D, and the force moment M. The forces calculated by a numerical simulation is also shown in the figure, where $\boldsymbol{\theta}$ obtained from the experiment and its derivatives $\dot{\boldsymbol{\theta}}$ and $\ddot{\boldsymbol{\theta}}$ are substituted into Eq. (1) of the simple method. In the mathematical model, the thoracic angle θ_t is specified at $10°$so as the lift becomes resembled by the experimental result. The angle reduction is reasonable because the effective inflow angle to the wings, i.e., attack-of-angle, in the experiment becomes smaller because of the induced downwash of wing tip vortices, the wing torsion, etc.

There are large differences in the drag especially at the circles as shown in Fig. 4. A result of the basic vortex method is similar to the simple method whereas the result is not shown here. It is considered that the difference in the drag appears since the interaction of the flow by the right-and-left wings is not contained in the mathematical model. The mathematical model will be reviewed and modified in the following section.

3.4.2. Observation

The flow around wings is visualized by a smoke wire as shown in Fig. 5. The figure (a) at $t = 0.04$ s shows that the airflow passes along the wing during downstroke of wings. This result gives the foundation that the dynamic pressure on the wing can be calculated by the Kutta-Joukowski theorem.

The figure (b) is of the same wing fixed in the steady flow with the equivalent attack-of-angle. The flow running upper wing surface is separated at the leading edge and the wing is stalled. It is clear that the airflow at the flapping of wings is greatly different from the steady state.

Fig. 6 is the side and back view to see the wake from the wing tip. Strong wing tip vortex wakes are observed during the flapping-of-wings motion.

4. Effects of Flapping-of-Wings

The experimental results show the characteristic aerodynamics at wingbeat phase and peeling phase. There exist strong wing tip vortex wakes that might have an effect on aerodynamics. Hence, the above fundamental

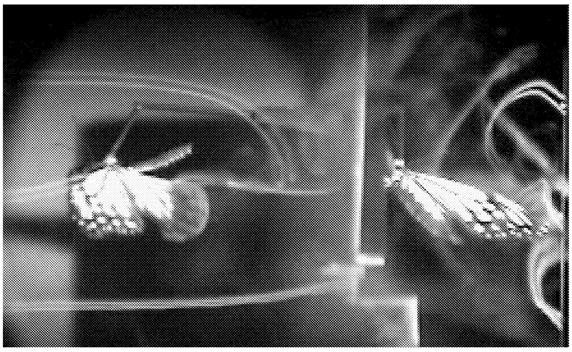

Figure 6: Strong wing tip vortex wakes

computation methods are not sufficiently accurate for aerodynamic modeling of the flapping-of-wings. The aerodynamics is reviewed and modified below.

4.1. Review of aerodynamics

The following effects are modeled and contained in the vortex method. The vortex method is considered here because those effects other than a damming effect need strength of bound vortex of wing. The following effects are computed for each instant because the relative position and orientation of the wings is varying.

4.1.1. Interaction of right-and-left wings

The bound vortex of each wing element induces velocity field around the wing. The wing sometimes locates in the velocity field induced by the other wing because of the flapping motion. In this case, the strength of the bound vortex should be determined considering the induced velocity.

4.1.2. Damming effect

At the wingbeat phase, the airflows around wings interact with each other and the airflow in between the right-and-left wings is dammed. The damming causes aerodynamic forces especially the drag of this phase. This damming effect of the wingbeat phase is modeled and an aerodynamic force is computed from the momentum change of the dammed air.

4.1.3. Downwash induced by wing tip vortices

A finite wing necessarily generates wing tip vortex wakes. The wing tip vortex wakes induce a velocity component called a downwash that effectively decreases the attack-of-angle. Differing from a fixed wing, its effect is time varying because of the flapping motion.

The strong wing tip vortex wakes are observed in the experiment, the downwash is contained in the model. The vortex wakes continuously leave from the wing tips. They are modeled as a superposition of many horseshoe vortices based on Prandtl's lifting-line theory. The induced velocity of the wing tip vortices are considered in the same manner as the interaction of the right-and-left wings.

4.1.4. Peel mechanism

At the start of downstroke, the overlapping right-and-left wings are peeled from the leading edges with elastic deformation. This is called a peel mechanism that may generate some thrust. The deformation of each wing is described by two plates at an angle with each other. The peel mechanism is then modeled as the backward movement of the nodal line. Some thrust is calculated by applying the vortex method to the wing of the two plates with appropriate boundary conditions.

4.2. Numerical simulations

The interaction of right-and-left wings and the damming effect is contained in the fundamental vortex method. After that, the effect of the downwash caused by the wing tip vortices is evaluated by the lifts in Fig. 7. The consideration of the wing tip vortices obtains the model closer to the experimental result.

In addition to the above model, the peel mechanism is evaluated by the drag in Fig. 8. The consideration of the peel mechanism obtains the model closest to the experimental result.

The proposed model with all the flapping-of-wings effects is shown in Fig. 9 together with the simple method, and the experiment. Accordingly, we have the considerably accurate model. The force moment about the fixed point of the proposed model is not in good agreement. There might be some effects that are not considered in the model.

5. Flapping Trajectory Search

Although the simulation is performed using the control torque calculated from the experiment, the mathematically modeled butterfly cannot fly. The control forces must be searched for a steady flapping-of-wings flight of the mathematical model.

The steady flapping-of-wings flight is defined as "all other than x of states $\boldsymbol{\theta}_f$ and $\dot{\boldsymbol{\theta}}_f$ after a flapping-of-

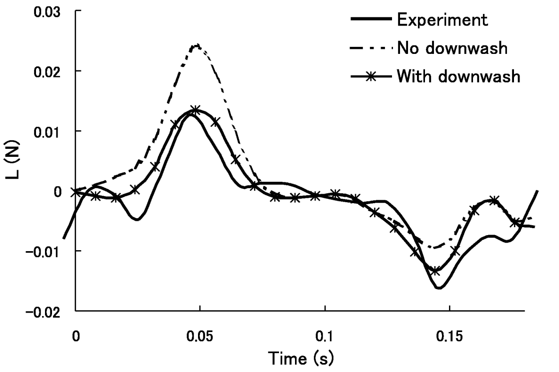

Figure 7: Effect of downwash caused by wing tip vortices

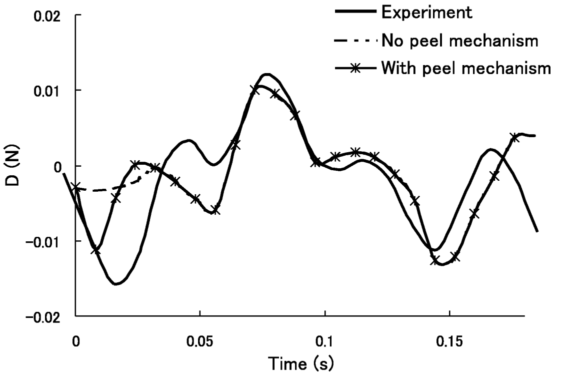

Figure 8: Effect of peel mechanism

wings period T are in agreement with initial value $\boldsymbol{\theta}_s$ and $\dot{\boldsymbol{\theta}}_s$."

A target orbit of the joint angle is generated by the dynamic associative memory(DAM) proposed by the present authors[3]. The DAM can generate any periodic motion within a specified approximation accuracy, which is based on a modulation method with a recurrent neural network oscillator and a layered neural network modulator. The parameters in the DAM and initial condition are considered as learning parameters to find a trajectory of the steady flapping-of-wings flight. For the reduced calculation time, number of parameters is cut down based on the knowledge from the experiment and the observation.

The following error function E is used for the learning evaluation:

$$E = \sum_i K_i(\theta_{if} - \theta_{is})^2 \qquad (5)$$

where i denotes z or θ_t or $\dot{x}$, and K_i is a constant number for appropriate scaling.

A gradient method finds the learning parameters in the above description such that the obtained trajectory

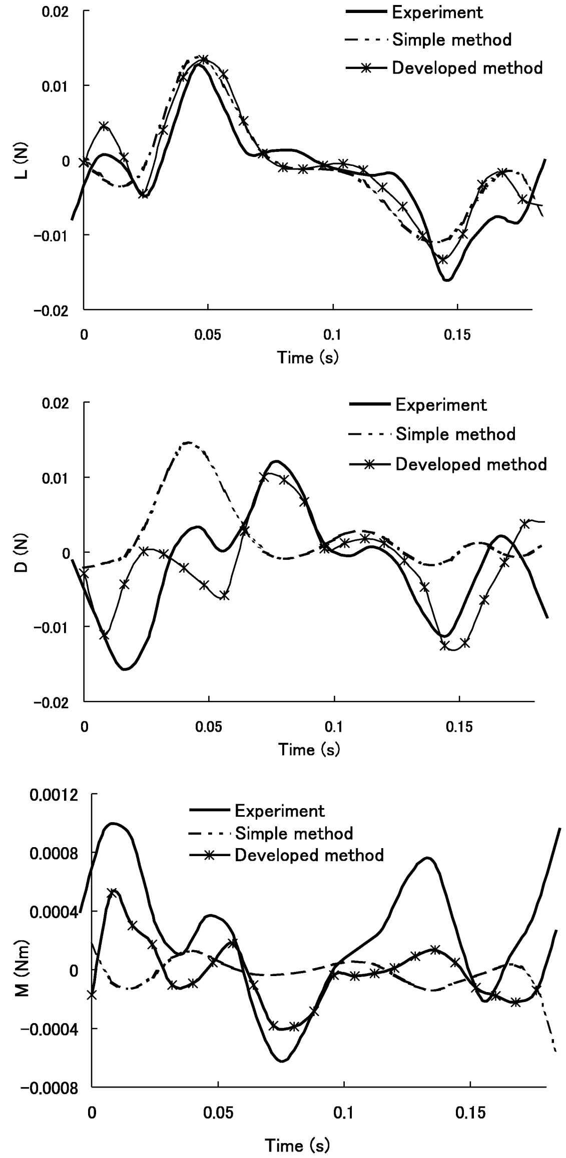

Figure 9: Proposed model, simple method, and experiment

satisfies the definition of the steady flapping-of-wings flight. We cannot find any trajectories that make the proposed model fly though we can find a trajectory for the simple method model. The proposed model may be more difficult to realize the longitudinal stability of the flapping-of-wings flight than the simple method model because the force moment of the proposed model varies in large through the flapping motion.

Fig. 10 illustrates an obtained result by using the simple method model. Though it doesn't perfectly correspond to the definition of steady flapping-of-wings flight, the obtained flapping trajectory is remarkably

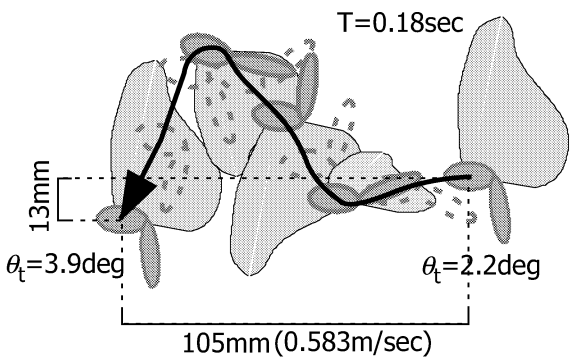

Figure 10: Flapping-of-wings flight of simple method model

similar to the trajectory of the experiment. When this motion is repeated, it gradually leaves from the periodic and steady flapping-of-wings flight and becomes unstable. The steady flapping-of-wings flight may be hopefully realized by easing the restriction of the parameter, modification of the mathematical model, etc.

6. Concluding Remarks

In order to clarify a stabilization phenomenon in flapping-of-wings flights, this study has performed the modeling of the butterfly, the experiment for the quantitative data acquisition and the qualitative observation, the simulator construction, and the comparison between the actual and the modeled butterfly. The simple method and the vortex method have been applied to make a simulator, where the methods calculates the aerodynamic force. Stability of flight has not shown in simulations yet. The stabilization will be hopefully realized by easing the restriction of the parameter, modification of the mathematical model, etc. But, some other effects, e.g., a feedback control, might be essential.

Acknowledgment

A part of this work is financially supported by a Grant-in-Aid for Scientific Research from Ministry of Education, Science, Culture, and Sports of Japan.

References

[1] Sunada, K. et al., "Performance of a Butterfly in Take-off Flight," *J. of Experimental Biology*, Vol. 183, pp. 249–277, 1993.

[2] Katz, J. and Plotkin, A., *Low-Speed Aerodynamics*, 2nd Ed., Cambridge University Press, Cambridge, 2001.

[3] Senda, K. and Tanaka, T., "Neural Motion Generator for Feedback Attitude Control of Space Robot," *Machine Intelligence and Robotic Control Journal*, Vol. 3, No. 3, pp. 129–136, 2001.